

## Electronic Supplementary Information (ESI)

### High-performance wearable supercapacitor based on PANI/N-CNT@CNT fiber with designed hierarchical core-sheath structure

*Jinyong Tian<sup>a</sup>, Nanjian Cui<sup>a</sup>, Peining Chen<sup>b</sup>, Kunkun Guo<sup>a</sup>, Xuli Chen<sup>a\*</sup>*

<sup>a</sup>College of Materials Science and Engineering, Hunan joint international laboratory of advanced materials and technology for clean energy, Hunan University, Changsha, 410082, P. R. China

<sup>b</sup>State Key Laboratory of Molecular Engineering of Polymers, Department of Macromolecular Science and Laboratory of Advanced Materials, Fudan University, Shanghai 200438, China

E-mail: [chenxuli@hnu.edu.cn](mailto:chenxuli@hnu.edu.cn)

### Experimental Section

#### 1. Preparation of N-CNTs on CNT fiber:

Catalyst of Fe (1.2 nm)/Al<sub>2</sub>O<sub>3</sub> (3 nm) on silicon wafer for spinnable CNT array was purchased from Tianjin Lattice Photoelectric Material Co. Ltd. Spinnable CNT array was synthesized by a typical CVD method with Fe (1.2 nm)/Al<sub>2</sub>O<sub>3</sub> (3 nm) on a silicon wafer as catalyst, ethylene as carbon source, and a mixture of Ar and H<sub>2</sub> gases as carrying gas. The CVD growth process was carried out in a quartz tube furnace. The growth temperature and growth time of CNT array were controlled as 740 °C and 10 min, respectively. After spinnable CNT arrays were synthesized, CNT fiber was spun from the as-synthesized CNT array. In more details, adhering a blade to the edge of a CNT array, CNT sheet was continuously pulled out of the array and subsequently spun

into fiber.

## 2. The calculation of fiber's electrical conductivity:

The conductivity ( $\sigma$ ) of the fiber electrode was calculated according to the definition<sup>S1-S3</sup>

$$\sigma = 1/\rho \quad (1)$$

where  $\rho$  is resistivity. Also according to the definition

$$\rho = R * S_s / L \quad (2)$$

where  $R$ ,  $S_s$  and  $L$  stand for the resistance, cross-section area and length of the fiber electrode tested, respectively. In the formula,  $R$  was tested by a ELIKE JC-890D+ digital multimeter,  $S_s$  was calculated by

$$S_s = \pi (D/2)^2 \quad (3)$$

where  $D$  is the diameter of the fiber.

## 3. Calculation of fiber electrode surface area:

The surface area of the fiber electrode was calculated by

$$S = \pi \times D \times L \quad (4)$$

where  $D$  and  $L$  are the diameter and length of the fiber electrode covered by the electrolyte.

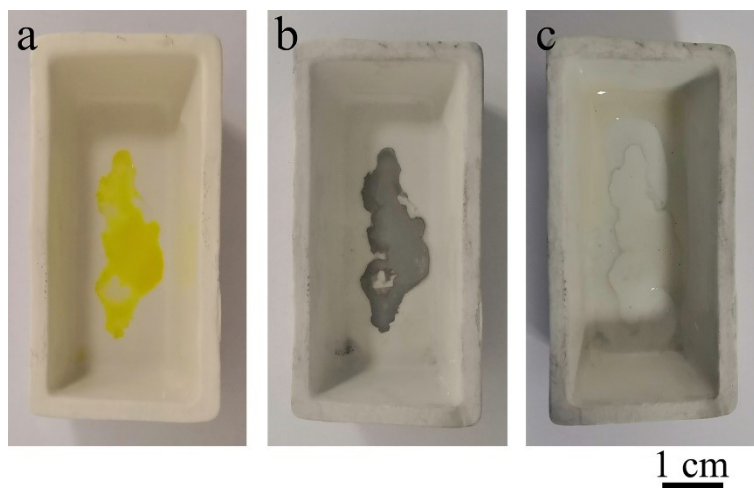


**Figure S1.** Ferric chloride (a) catalyst precursor solution, (b) reduced into iron during CVD process and (c) then dissolved in acid solution.

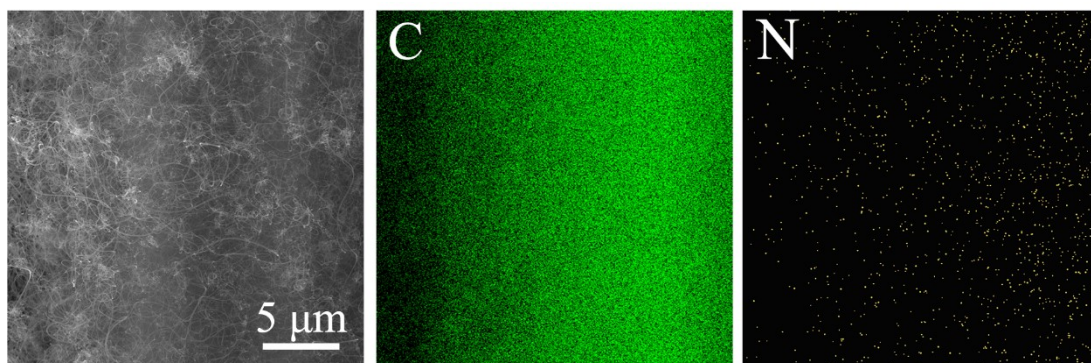


**Figure S2.** EDS mapping of N-CNT@CNT fiber composites.

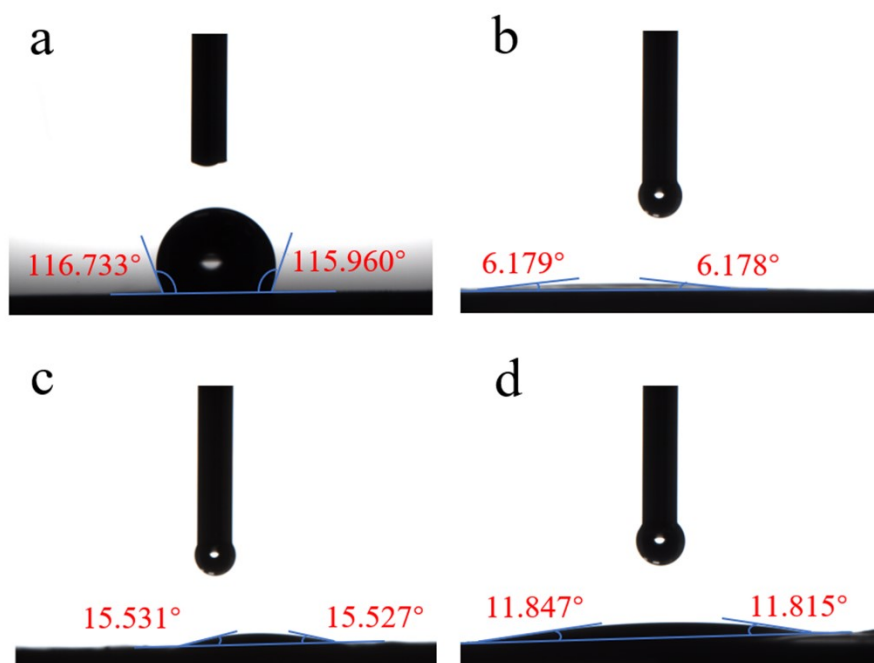


**Figure S3.** Static water contact angles on sheet electrodes with the same material structure of corresponding fiber electrodes. (a) CNT, (b) N-CNT@CNT, (c) PANI@CNT and (d) PANI/N-CNT@CNT.

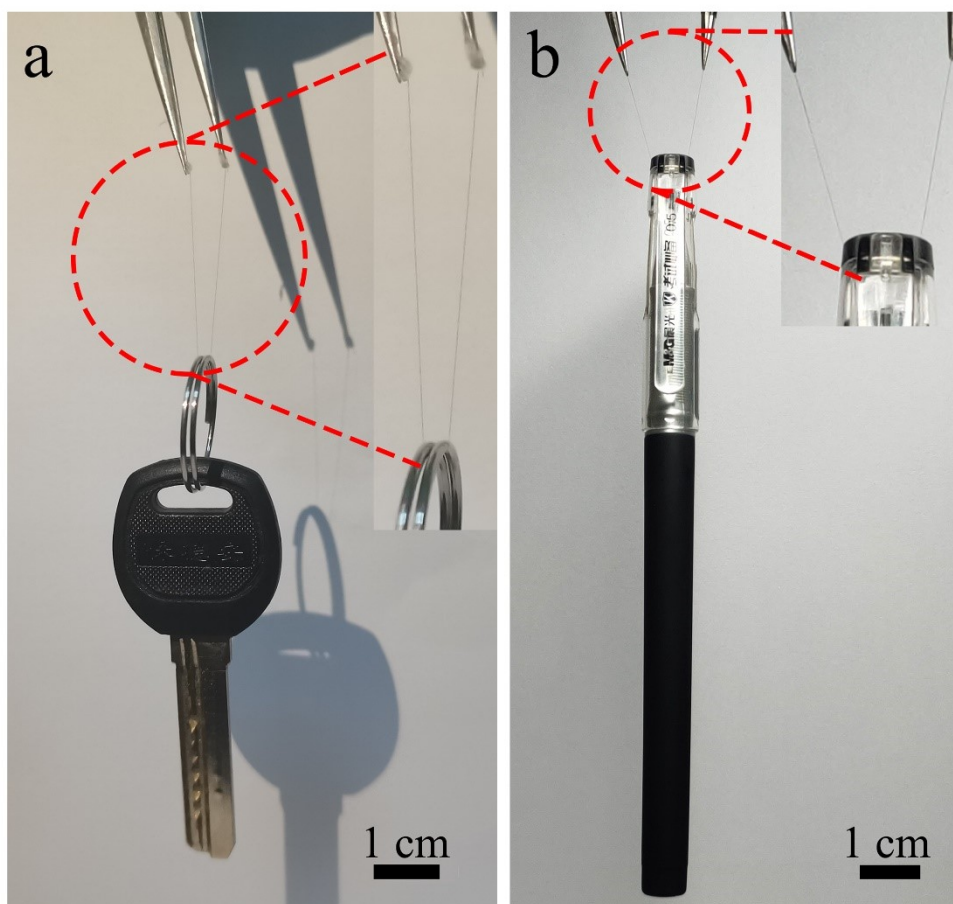


**Figure S4.** Optical images of N-CNT@CNT fiber lifting weights of a (a) key and (b) pen.

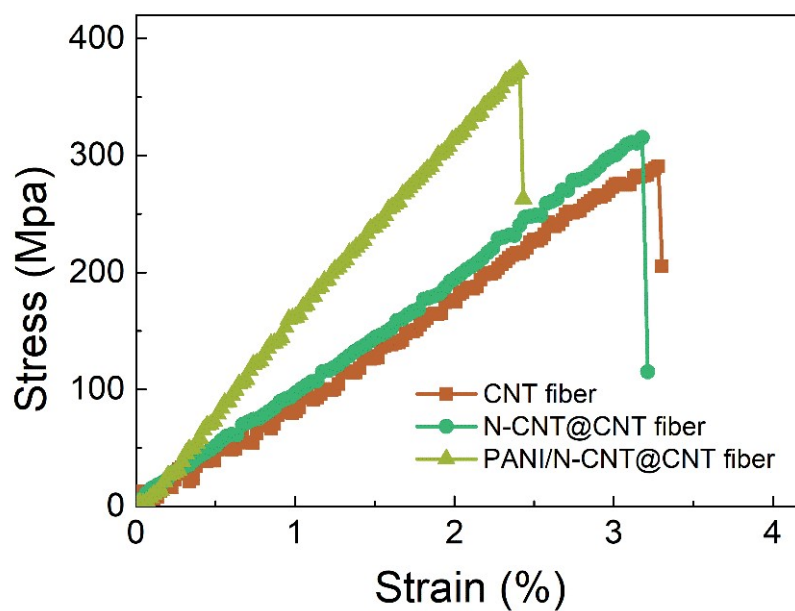


**Figure S5.** Typical tensile stress-strain curves for CNT fiber, N-CNT@CNT fiber and PANI/N-CNT@CNT fiber, respectively.

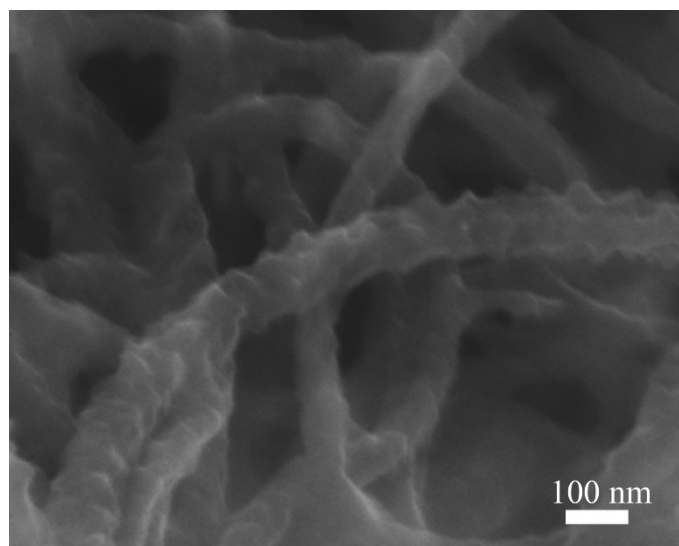


**Figure S6.** Magnified SEM image of PANI/N-CNT in PANI/N-CNT@CNT fiber.

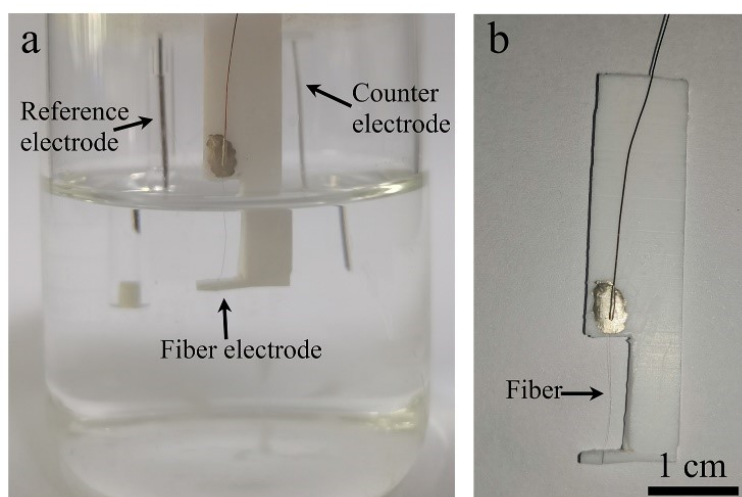


**Figure S7.** The optical photos of (a) fiber electrode in three-electrode system, (b) fiber electrode fixed on a plastic holder.

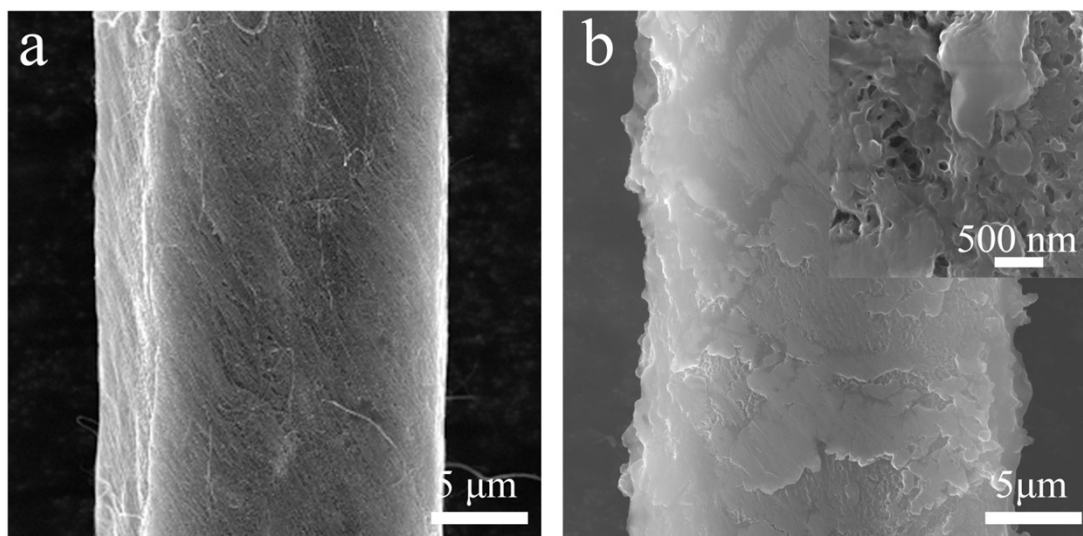


**Figure S8.** SEM images of (a) CNT fiber and (b) PANI@CNT fiber with 70% PANI, the inset in b is the magnified SEM image.

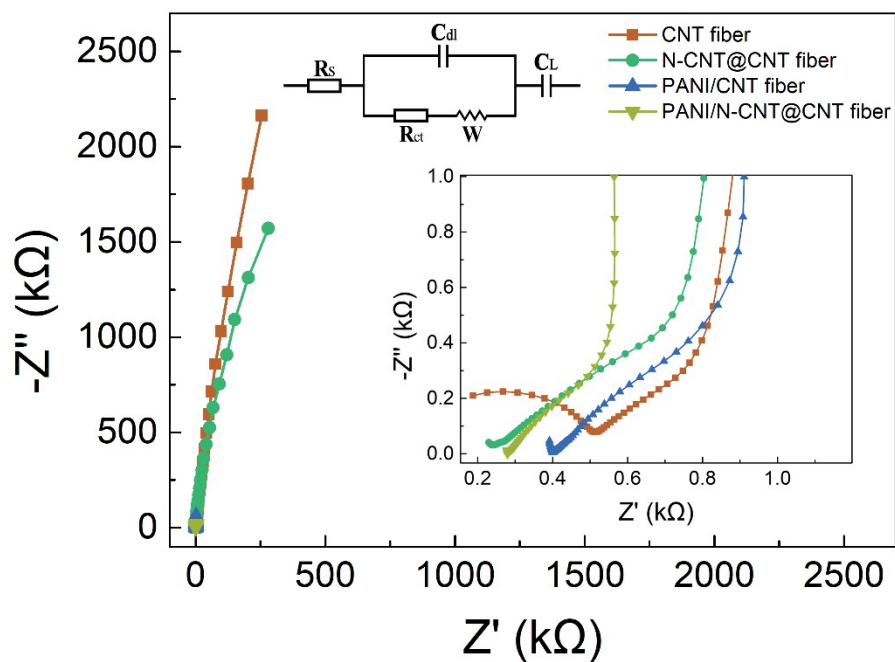


**Figure S9.** Nyquist plots of fiber electrodes with different structures. The insets are the Nyquist plots in the high-frequency region and the Equivalent circuit to fit the EIS data.<sup>60, S4</sup> The equivalent values of  $R_s$  and  $R_{ct}$  were summarized in Table S2.  $R_s$ ,  $R_{ct}$ ,  $W$ ,  $C_{dl}$  and  $C_L$  stand for the series resistance, charge transfer resistance, Warburg element, double-layer capacitance and pseudocapitance, respectively.

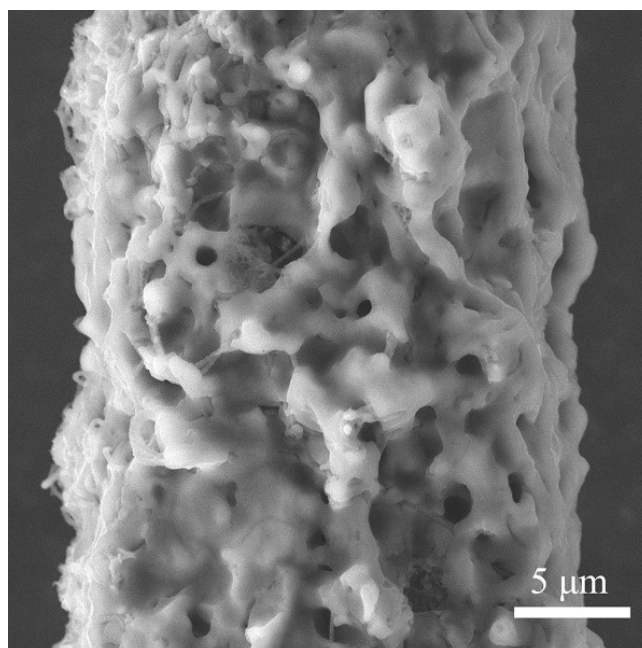


**Figure S10.** SEM images of PANI/N-CNT@CNT fiber with PANI weight percentage of 80%.

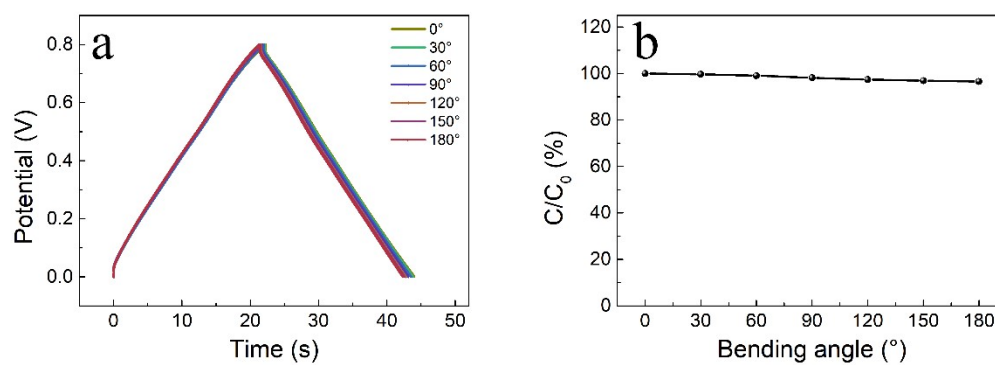


**Figure S11.** Electrochemical characterization of PANI/N-CNT@CNT fiber electrode under different bending angles. (a) GCD profiles of fiber electrode bending at different angles. (b) Capacitance retention of fiber electrode under different bending angles.

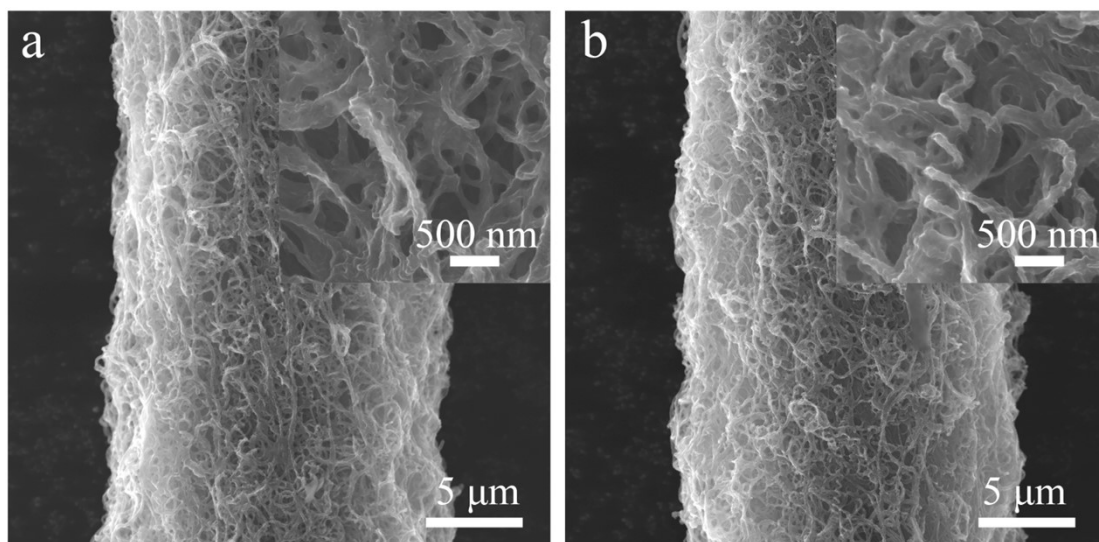


**Figure S12.** SEM images of PANI/N-CNT@CNT fiber electrode (a) before and (b) after 1000 cycles of GCD processes under  $10 \text{ A g}^{-1}$ , the insets are the corresponding SEM image under higher magnification.

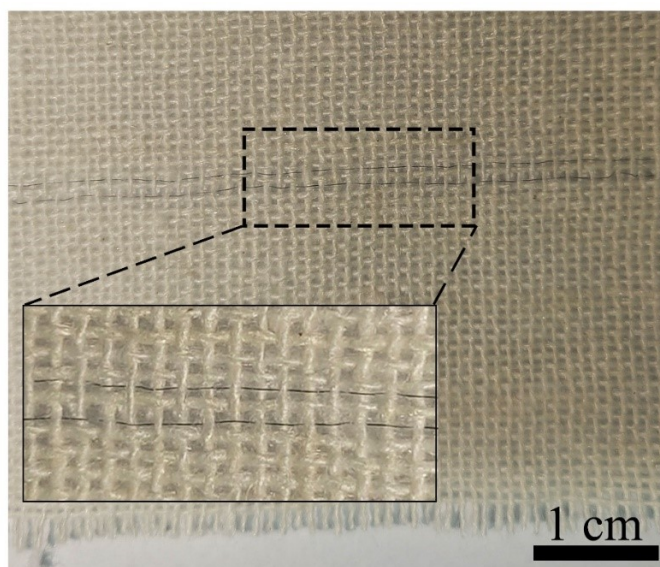


**Figure S13.** The picture of the hierarchical core-sheath fiber based supercapacitors woven into a textile.

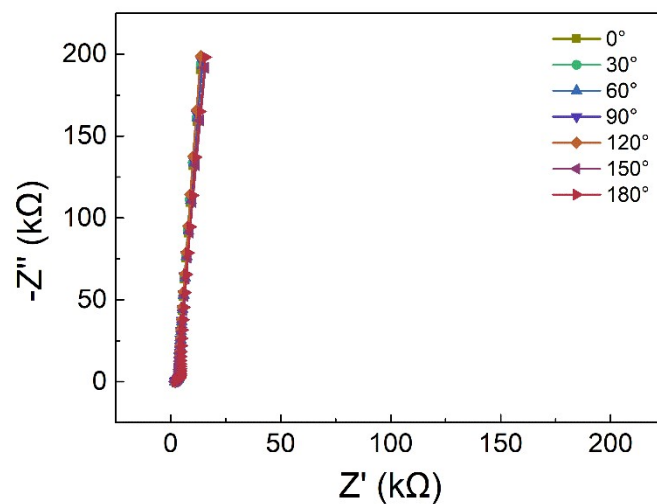


**Figure S14.** Nyquist plots of the FCS bending at different angles.

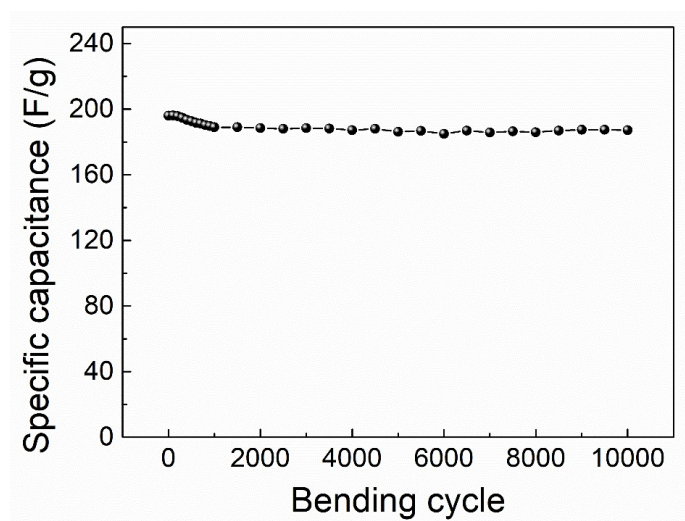


**Figure S15.** FSC capacitance values after different bending cycles of 0°-to-180°-to-0°.

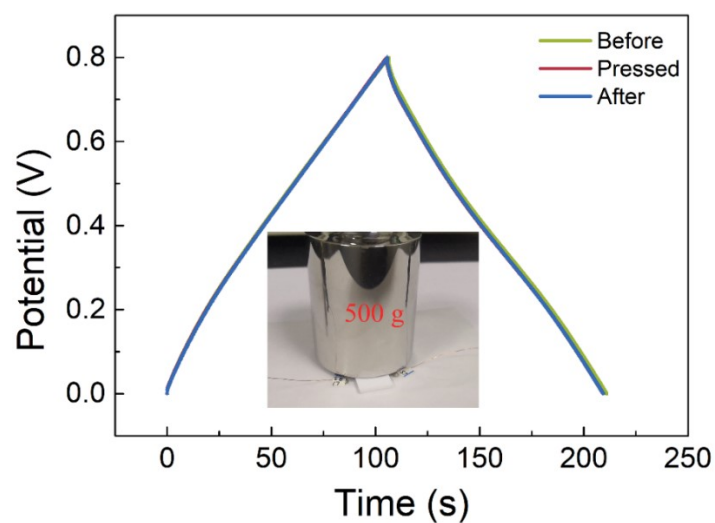


**Figure S16.** GCD profiles of the FCS before, during and after pressing process, and the inset is the

optical photograph of the test under compression.

**Table S1.** Surface area of fiber electrodes with length of 1 cm and the corresponding areal specific capacitance.

Fiber electrode	CNT fiber	N-CNT@CNT fiber	PANI@CNT fiber	PANI/N-CNT@CNT fiber
Surface area (cm <sup>2</sup> )	$4.71 \times 10^{-3}$	$7.76 \times 10^{-3}$	$5.97 \times 10^{-3}$	$7.85 \times 10^{-3}$
Areal specific capacitance (mF cm <sup>-2</sup> )	1.50	3.08	108.83	121.38

**Table S2.** Equivalent series resistance ( $R_s$ ) and charge transfer resistance ( $R_{ct}$ ) of the fiber electrodes with different structures.

Fiber electrode	CNT fiber	N-CNT@CNT fiber	PANI@CNT fiber	PANI/N-CNT@CNT fiber
$R_s$ ( $\Omega$ )	19	16	31	25
$R_{ct}$ ( $\Omega$ )	508	236	370	254

**Table S3.** Comparison of the Electrochemical Characteristics with Those Observed in Other Studies.<sup>20, 21, 25, 26, 55-62</sup>

	Electrode material	Electrolyte	Capacitance	Cycle life	Bending cycle life
<b>This work</b>	PANI/N-CNT@CNTF	PVA/H <sub>3</sub> PO <sub>4</sub>	264.8 F g <sup>-1</sup> (1 A g <sup>-1</sup> )	92.1% (10000 cycles)	95.5% (10000 cycles)
<b>58</b>	PANI/CNTF	PVA/H <sub>2</sub> SO <sub>4</sub>	221 F g <sup>-1</sup> (0.3 A g <sup>-1</sup> )	79.9% (10000 cycles)	85.6% (15000 cycles)
<b>59</b>	CNT-Au@OCNT-PANI	PVA/H <sub>3</sub> PO <sub>4</sub>	324 F cm <sup>-3</sup> (0.5 A cm <sup>-3</sup> )	80% (2000 cycles)	85% (3000 cycles)
<b>60</b>	CNTF/CNTs/PANI	PVA/H <sub>3</sub> PO <sub>4</sub>	67.31 mF cm <sup>-2</sup> (0.5 mA cm <sup>-2</sup> )	90% (5000 cycles)	99.8% (500 cycles)
<b>61</b>	CNT/PANI	PVA/H <sub>3</sub> PO <sub>4</sub>	394 F g <sup>-1</sup> (2mV s <sup>-1</sup> )	75.7% (12000 cycles)	—
<b>55</b>	PANI@CNT/G	PVA/H <sub>3</sub> PO <sub>4</sub>	138 F g <sup>-1</sup> (1 A g <sup>-1</sup> )	77.3% (5000 cycles)	—

			<sup>1)</sup>	cycles)	
25	CNT/PANI	PVA/H <sub>3</sub> PO <sub>4</sub>	111.6 F g <sup>-1</sup> (0.5 A g <sup>-1</sup> )	90% (2000 cycles)	95.2% (5000 cycles)
21	CNT/PANI	PVA/H <sub>3</sub> PO <sub>4</sub>	255.5 F g <sup>-1</sup> (1 A g <sup>-1</sup> )	69% (10000 cycles)	94% (1000 cycles)
56	IR-CNT@PANI	PVA/H <sub>3</sub> PO <sub>4</sub>	78 F g <sup>-1</sup> (2 A g <sup>-1</sup> )	89% (1000 cycles)	98% (200 cycles)
57	CNT/PANI	PVA/H <sub>3</sub> PO <sub>4</sub>	272.7 F g <sup>-1</sup> (1 A g <sup>-1</sup> )	90% (2000 cycles)	96.4% (200 cycles)
62	PANI/CNT	PVA/H <sub>2</sub> SO <sub>4</sub>	6.23 mF cm <sup>-2</sup> (0.2 A g <sup>-1</sup> )	86% (800 cycles)	–
26	PANI/CNTF	PVA/H <sub>3</sub> PO <sub>4</sub>	274 F g <sup>-1</sup> (1 A g <sup>-1</sup> )	–	97% (50 cycles)
20	PANI/CNTF	PVA/H <sub>2</sub> SO <sub>4</sub>	38 mF cm <sup>-2</sup> (0.01 mA cm <sup>-2</sup> )	91% (800 cycles)	–

## References

- [S1] Hao Sun, Xiao You, Jue Deng, Xuli Chen, Zhibin Yang, Jing Ren and Huisheng Peng, *Adv. Mater.*, 2014, **26**, 2868-2873.
- [S2] Zhuanpei Wang, Jianli Cheng, Qun Guan, Hui Huang, Yinchuan Li, Jingwen Zhou, Wei Ni, Bin Wang, Shi He, Huisheng Peng, *Nano Energy*, 2018, **45**, 210–219.
- [S3] Guangxi Huang, Ye Zhang, Lie Wang, Peng Sheng, Huisheng Peng, *Carbon*, 2017, **125**, 595-604.
- [S4] Yiliang Wang, Huaqiang Xuan, Gaoxin Lin, Fan Wang, Zhi Chen, Xiaoping Dong, *J. Power Sources*, 2016, **319**, 262-270.